

Model Based Predictive Direct Torque and Flux Control for Grid Synchronization of a PMSG Driven by a Direct Matrix Converter

Badreddine Babes
*Research Center in Industrial
 Technologies (CRTI)*
 Algiers, Algeria
 elect_babes@yahoo.fr

Oualid Aissa
*LPMRN Laboratory
 Faculty of Sciences and Technology
 University of Bordj Bou Arreridj*
 Bordj Bou Arreridj, Algeria
 oualid.aissa@univ-bba.dz

Noureddine Hamouda
*Research Center in Industrial
 Technologies (CRTI)*
 Algiers, Algeria
 n.hamouda@crti.dz

Ilhami Colak
*Faculty of Engineering and
 Architecture*
Nisantasi University
 Istanbul, Turkey
 ilhcol@gmail.com

Abstract—We have proposed in this article a recent intuitive approach which concerns a Direct Matrix Converter (DMC), intended for the optimal power control of a Wind Energy Conversion System (WECS) with a Permanent Magnets Synchronous Generator (PMSG). The future switching state of the DMC is performed by a simple-cost optimization algorithm for a discrete system model without the need for additional modulation block or cascaded control loops. The control objectives are regulation of the mechanical torque and flux of the PMSG according to an arbitrary references established based on the maximum power point tracker (MPPT), in addition a proper tracking of the output reactive power to its reference ensuring unitary power factor. Simulation was used to study and test the whole control system. The results obtained are very satisfactory, ensuring better control of the WECS thanks to the use of the DMC structure.

Keywords—Intuitive approach, PMSG, wind, direct matrix converter (DMC), simulation results

I. INTRODUCTION

The permanent magnet synchronous generator (PMSG), which is characterized by its robustness and ease of maintenance, has several benefits in variable speed operation as well as medium and high power applications [1]. The power electronics interface, which typically consists of a two-stage AC-DC-AC converter system, is coupled between the wind generator and the power grid to be applied only at a restricted speed range and rated at a fraction of the machine's nominal power [2].

In recent years, the use of direct AC-AC frequency power converters, such as DMC and indirect matrix converter (IMC), has gained wide acceptance. In the AC drives, these structures ensure sinusoidal currents for AC-AC conversion [3]. The matrix converter (MC) in turn ensures the advantages of low distortion of input and output currents with adjustable amplitude and frequency; a bidirectional power flow and unity power factor when operating in motor and regenerative modes. Among the favorable characteristics of the MC is the bulky absence of the DC-link energy storage component thus allowing the ability to operate under adverse atmospheric conditions. These peculiarities make the MC an appropriate solution for

high efficiency converters, which have invaded different important fields, including military, variable speed operation of wind energy systems, aerospace, compact motor drives and skin pass mill. However, the main disadvantage of this solution is the difficulty of control.

Newly published research papers have discussed the control of PMSG-based wind power generation systems [4-6]. These researches have focused on the development of control techniques in order to bring about substantial improvements in the production system [7, 8]. In the literature, only a few articles have discussed the introduction of MCs in the wind generation systems [9].

From the new control strategies for power converters developed in the last years, the use of Model Predictive Control (MPC) is a very interesting alternative due to its intuitive concept, simple principle, good dynamic behavior and flexibility [10-13]. The MPC allows to control several different variables of a system taking into account constraints and nonlinearities [14, 15].

The objective sought for this article consists in the study of the advantages of the predictive algorithm and the DMC simultaneously. The expected result of this research work is characterized by a simple, intuitive and new control of the electromagnetic torque and the stator flux of the PMSG. On the other hand, a substantial improvement in the control scheme is ensured by the introduction of a reactive power minimization strategy which will in turn guarantee a power factor close to unity on the grid side of the MC converter. The results obtained by MATLAB/Simulink package program confirm the effectiveness of the proposed control approach.

The presented work is structured as follows: section II presents the overall system description; section III describes the mathematical model of the PMSG; section IV exhibits the direct matrix converter; sections V and VI depict respectively the proposed advanced control strategy and the obtained simulation results. Finally, conclusions are given in section VII.

II. DESCRIPTION OF THE STUDIED SYSTEM

A three phase direct matrix converter, used as an interface between the PMSG and utility grid via an output power filter, is shown in Fig. 1. The input side of the DMC is controlled effectively for variable speed operation of the PMSG to enable the maximum power extraction from the available wind. The output side of the DMC controls the reactive power exchange between the wind generator and the power grid.

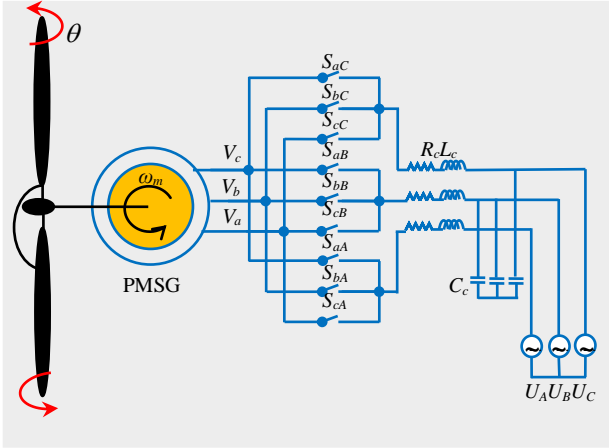


Fig. 1. Schematic representation of the wind PMSG with DMC.

III. PMSG MODELING

For surface mounted PMSG modeling, a fifth order dynamic model is used in this paper [16, 17]. The generator equations in a stationary reference frame can be described by using complex vectors as follows [18]:

$$V_s = R_s i_s + \frac{d\Psi_s}{dt} \quad (1)$$

$$\Psi_s = L_s i_s + \Psi_r \quad (2)$$

$$\Psi_r = \Psi_f e^{j\theta_e} \quad (3)$$

$$T_e = \frac{3}{2} p \Im(\bar{\Psi}_s i_s) \quad (4)$$

$$J \frac{d\omega_r}{dt} = T_e - T_m + F\omega_m \quad (5)$$

Where V_s is the stator voltage (V), i_s is the stator current (A), R_s is the generator resistance (Ω), Ψ_s is the stator vector flux (Wb), Ψ_r is the rotor flux vector (Wb), the inductances of d - q axes are equal ($L_q=L_d=L_s$), ω_e is the electrical speed (rad/s), θ_e is the electrical position ($d\theta_e/dt=\omega_e$), Ψ_f is the magnet flux (Wb), p is the pair of poles, F is the rotational friction ($kg\ m^2/s$), J is the total rotational inertia of the system ($kg\ m^2$), and T_m is the mechanical torque produced by the turbine (Nm).

IV. DYNAMIC MODEL OF THE DMC

The single-stage AC-AC direct matrix power converter is composed of nine insulated-gate bipolar transistors (IGBT), whose control is bidirectional. This kind of converter connects directly the power source to the load where its operation is based on twenty seven switching states [19]. This number of switching states delivered according to the restriction of the DMC structure under the

following conditions: non-shortening of the input terminals and requirement of non-opening of the output phase. Table I includes the different allowable switching states of the DMC 3×3 which are classified into three groups based on the input current vector and the output voltage type [20].

TABLE I. PERMITTED SWITCHING STATES OF DMC

Group states	Phase	Output voltage	Input current	Switching function values									
				ABC	$U_{AB}U_{BC}U_{CA}$	$i_{ia} i_{ib} i_{ic}$	$S_{bA}S_{aB}S_{cC}S_{bB}S_{aC}S_{cB}S_{cA}S_{cB}S_{cC}$						
I	i	abc	$U_{AB}U_{BC}U_{CA}$	$i_{ia} i_{ib} i_{ic}$	1	0	0	0	1	0	0	0	1
	ii	acb	$-U_{AB}-U_{BC}-U_{CA}$	$i_{ia} i_{ic} i_{ib}$	1	0	0	0	0	1	0	1	0
	iii	bac	$-U_{AB}-U_{CA}-U_{BC}$	$i_{ib} i_{ia} i_{ic}$	0	1	0	1	0	0	0	0	1
	iv	bca	$U_{CA}U_{CA}U_{AB}$	$i_{ic} i_{ia} i_{ib}$	0	1	0	0	0	1	1	0	0
	v	cab	$U_{AB}U_{AB}U_{BC}$	$i_{ib} i_{ic} i_{ia}$	0	0	1	1	0	0	0	1	0
	vi	cba	$-U_{BC}-U_{AB}-U_{CA}$	$i_{ic} i_{ib} i_{ia}$	0	0	1	0	1	0	1	0	1
AII	i	acc	$U_{CA}0U_{CA}$	$i_{ia}0 -i_{ia}$	1	0	0	0	0	1	0	0	1
	ii	bcc	$-U_{BC}0-U_{BC}$	$0 i_{ia} -i_{ia}$	0	1	0	0	0	1	0	0	1
	iii	baa	$-U_{AB}0U_{AB}$	$-i_{ia} i_{ia}0$	0	1	0	1	0	0	1	0	0
	iv	caa	$U_{CA}0-U_{CA}$	$-i_{ia}0 -i_{ia}$	0	0	1	1	0	0	1	0	0
	v	cbb	$-U_{BC}0U_{BC}$	$0 -i_{ia} -i_{ia}$	0	0	1	0	1	0	0	1	0
	vi	abb	$U_{AB}0-U_{AB}$	$U_{AB}0 -i_{ia}0$	1	0	0	0	1	0	0	1	0
IIB	i	cac	$U_{CA}-U_{CA}0$	$i_{ib}0 -i_{ib}$	0	0	1	1	0	0	0	0	1
	ii	cbc	$-U_{BC}-U_{BC}0$	$0 i_{ib} -i_{ib}$	0	0	1	0	1	0	0	0	1
	iii	aba	$U_{AB}-U_{AB}0$	$-i_{ib} i_{ib}0$	1	0	0	0	1	0	1	0	0
	iv	aca	$-U_{CA}U_{CA}0$	$-i_{ib}0 i_{ib}$	1	0	0	0	0	1	1	0	0
	v	ccb	$U_{BC}-U_{BC}0$	$0 -i_{ib} i_{ib}$	0	1	0	0	0	0	1	0	1
	vi	bab	$-U_{AB}U_{AB}0$	$i_{ib} -i_{ib}0$	0	1	0	1	0	0	0	1	0
IIC	i	cca	$0-U_{CA}-U_{CA}$	$i_{ic}0 -i_{ic}$	0	0	1	0	0	1	1	0	0
	ii	ccb	$0-U_{BC}-U_{BC}$	$0 i_{ic} -i_{ic}$	0	0	1	0	0	1	0	1	0
	iii	aab	$0U_{AB}-U_{AB}$	$-i_{ic} i_{ic}0$	1	0	0	1	0	0	0	1	0
	iv	aac	$0-U_{CA}U_{CA}$	$-i_{ic}0 i_{ic}$	1	0	0	1	0	0	0	0	1
	v	bbc	$0U_{BC}-U_{BC}$	$0 -i_{ic} i_{ic}$	0	1	0	0	1	0	0	0	1
	vi	bba	$0-U_{AB}U_{AB}$	$i_{ic} -i_{ic}0$	0	1	0	0	1	0	1	0	0
II	i	aaa	0 0 0	0 0 0	1	0	0	1	0	0	1	0	0
	ii	bbb	0 0 0	0 0 0	0	1	0	0	1	0	0	1	0
	iii	ccc	0 0 0	0 0 0	0	0	1	0	0	1	0	0	1

The DMC includes an $R_f L_f C_f$ power filter on the output side, useful for overcoming high voltages and decreasing harmonic distortion caused by switching and the inductive nature of the AC network. It is considered as a 2nd order system as given by these mathematical relations:

$$\dot{i}_s(t) = L_f^{-1} (V_s(t) - V_i(t)) - R_f L_f^{-1} i_s(t) \quad (6)$$

$$\dot{V}_i(t) = C_f^{-1} (i_s(t) - i_i(t)) \quad (7)$$

Where L_f is the inductance, R_f the damping resistor and C_f the capacitor of the output power filter.

Based on the equations presented above, the output can be given by a state space form with the internal variables i_i and V_i :

$$\begin{bmatrix} \dot{i}_s \\ \dot{V}_i \end{bmatrix} = A \begin{bmatrix} i_i \\ V_i \end{bmatrix} + B \begin{bmatrix} i_s \\ V_s \end{bmatrix} \quad (8)$$

Where A and B are matrices of appropriate dimensions.

$$A = \begin{bmatrix} 0 & 1/C_f \\ -1/L_f & R_f \end{bmatrix}, \quad B = \begin{bmatrix} 0 & -1/C_f \\ 1/L_f & 0 \end{bmatrix} \quad (9)$$

V. PREDICTIVE CONTROL STRATEGY

The suggested Predictive Direct Torque Control (PDTTC) scheme for the direct drive PMSG is illustrated by Figure. 2. The approach aims of selecting one of the twenty seven existing switch states of the DMC that brings the rotor torque T_e and the stator flux Ψ_s closest to their imposed values at fixed sampling time period while minimizing the

reactive power Q_o on the output side of the DMC. Figure 3 represents the flowchart of the designed PDTC in this paper. For this research work, the external PI type regulator generates the torque setpoint T_{ref} and control the PMSG speed. This same torque reference will be deployed to provide the trigger patterns to extract the maximum mechanical power from the wind turbine. On the other hand, the role of the PI regulator is to achieve zero stable state error thanks to its integral part [21]. Thereby, the fast dynamics of the PDTC approach can be seen simply as a unit gain between the reference and the controlled variables.

A. Flux Estimation

Non-measurable variables are calculated by an estimation block, such as the stator flux ψ_s and the rotor flux ψ_r . In PDTC, estimations of the stator flux ψ_s and the rotor flux ψ_r are indispensable for the present sampling phase $t(k)$. The stator flux estimation can be calculated using the stator voltage equation of the PMSG presented in (1). Thanks to the forward difference Euler formula to discretize (1), the stator flux calculation can be calculated as below:

$$\psi_s(k) = \psi_s(k-1) + T_s V_s(k) - R_s i_s(k) \quad (10)$$

Where T_s is the sampling period.

Based on the equivalent equation of the PMSG stator dynamics which is given in the form of standard state space, one can easily calculate the rotor flux as follows:

$$\frac{di_s}{dt} = \frac{1}{L_s} (V_s - R_s i_s - j\omega \psi_r) \quad (11)$$

Discretizing (11), and replacing the derivatives by the Euler based backwards approximation, the rotor flux calculation $\psi_r(k)$ is given:

$$\psi_r(k) = \frac{1}{L_s T_s} [i_s(k) - i_s(k-1)] - V_s(k) + R_s i_s(k) \quad (12)$$

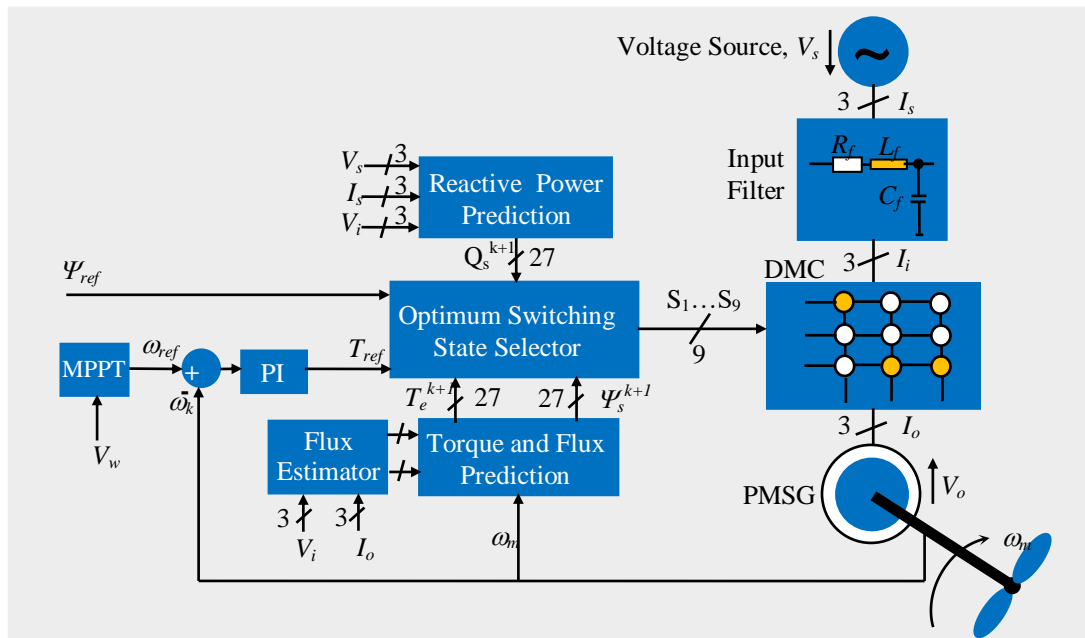


Fig. 2. Developed intuitive DTC for the wind PMSG.

B. Predictive Torque and Flux Variables

Once the estimates of the rotor and stator fluxes are established, the calculation of the predictions of these variables is necessary. In the case of PDTC, the stator flux $\psi_s(k)$ and the electromagnetic torque $T_e(k)$ are predicted for the $t(k+1)$. The stator flux and the electromagnetic torque prediction variables can be calculated according (13) and (14).

$$\psi_s(k+1) = \psi_s(k) + T_s V_s(k+1) - R_s T_s i_s(k+1) \quad (13)$$

$$T_e(k+1) = \frac{3}{2} p \Im m [\bar{\psi}_s(k+1) i_s(k+1)] \quad (14)$$

As observed in (13) and (14), the prediction of these quantities is subordinate to the prediction of the stator current $i_s(k+1)$.

For this reason, the predicted relation of the stator current $i_s(k+1)$ is determined thanks to the equivalent equation of the stator dynamics of the PMSG presented in (1):

$$i_s(k+1) = \frac{T_s}{L_s} [V_s(k+1) - R_s i_s(k) - j\omega \psi_r(k+1)] + i_s(k) \quad (15)$$

C. Instantaneous Reactive Power Prediction

A discrete time state space representation of the output side for a sampling time T_s can be employed to predict the internal behavior of the output current considering the capacitor voltages and output current measurements at the k^{th} sampling time. The discrete time equivalent system of (8), when the input is generated by a zero order hold and all matrices are constant is given by:

$$\begin{bmatrix} i_i(k+1) \\ V_i(k+1) \end{bmatrix} = \varphi \begin{bmatrix} i_i(k) \\ V_i(k) \end{bmatrix} + \gamma \begin{bmatrix} i_s(k) \\ V_s(k) \end{bmatrix} \quad (16)$$

Where:

$$\varphi = \begin{bmatrix} \varphi_{11} & \varphi_{12} \\ \varphi_{21} & \varphi_{22} \end{bmatrix} = e^{AT_s}, \quad \gamma = \begin{bmatrix} \gamma_{11} & \gamma_{12} \\ \gamma_{21} & \gamma_{22} \end{bmatrix} = \int_0^{T_s} e^{A\tau} B d\tau = A^{-1}(\varphi - I_{2 \times 2})B \quad (17)$$

Assuming that:

$$\left. \begin{aligned} V_s(t) &= V_s(kT_s) = V_s(k) \\ i_e(t) &= i_e(kT_s) = i_e(k) \end{aligned} \right\} \text{for } kT_s \leq t \leq (k+1)T_s \quad (18)$$

Thus, the output current and capacitor voltage can be expressed by (19) and (20).

$$i_s(k+1) = \varphi_{21}V_i(k) + \varphi_{22}i_s(k) + \gamma_{21}V_s(k) + \gamma_{21}i_i(k) \quad (19)$$

$$V_i(k+1) = \varphi_{11}V_i(k) + \varphi_{12}i_s(k) + \gamma_{11}V_s(k) + \gamma_{12}i_i(k) \quad (20)$$

The prediction of output instantaneous reactive power is established through the future state of the output current and grid voltage as presented in (21):

$$\begin{aligned} Q_s(k+1) &= \text{Im} \left[V_s(k+1) \bar{i}_s(k+1) \right] \\ &= V_{s\beta}(k+1) i_{s\alpha}(k+1) - V_{s\alpha}(k+1) i_{s\beta}(k+1) \end{aligned} \quad (21)$$

Where the subscripts α and β are the real and imaginary components of the associated vector. We identify grid voltages as low frequency signals while assuming that: $V_s(k+1) \approx V_s(k)$.

D. Cost Functions Calculation

In order to decide on the best switching state to apply, the quality function is authorized to offer the evaluation criteria.

The cost function $g_i(k+1)$ is identified by the combination in a single term of the predicted torque with its nominal value and of the predicted flux corresponding to the reference flux.

$$g_i(k+1) = \frac{|T_{ref} - T_e(k+1)_h|}{T_n} + \lambda_{\psi} \frac{\|\psi_{ref}\| - \|\psi_s(k+1)_h\|}{\|\psi_s\|_{nom}} \quad (22)$$

$$i = 1, 2, 3, \dots, 27.$$

Where λ_{ψ} denotes a weight factor of the cost function. The adjustment of this factor whose role serves to increase or decrease the importance of the flux control compared to the torque control.

Among the essential advantages offered by the DMC, we will cite the possibility of controlling the displacement factor on the mains side with minimization of the output reactive power. At the same time multiple objectives can be achieved by adding more functions in the global cost function $g_i(k+1)$.

By adding a third term to the cost function of (22), we can easily have the resulting cost function of (23) including both objectives:

$$\begin{aligned} f_i(k+1) &= \frac{|T_{ref} - T_e(k+1)_h|}{T_n} + \lambda_{\psi} \frac{\|\psi_{ref}\| - \|\psi_s(k+1)_h\|}{\|\psi_s\|_{nom}} \dots \\ &+ \lambda_q |v_s^{\alpha}(k+1)i_s^{\beta}(k+1) - v_s^{\beta}(k+1)i_s^{\alpha}(k+1)|, i = 1, 2, 3, \dots, 27. \end{aligned} \quad (23)$$

The weighting factor λ_q handles the relevance of this term to the other terms in the cost function. At every sampling interval, and for all 27 valid switching states of the DMC, the cost function is evaluated, and the commutation state that produces the smallest value of $f_i(k+1)$ is selected to actuate the DMC in the next sampling period.

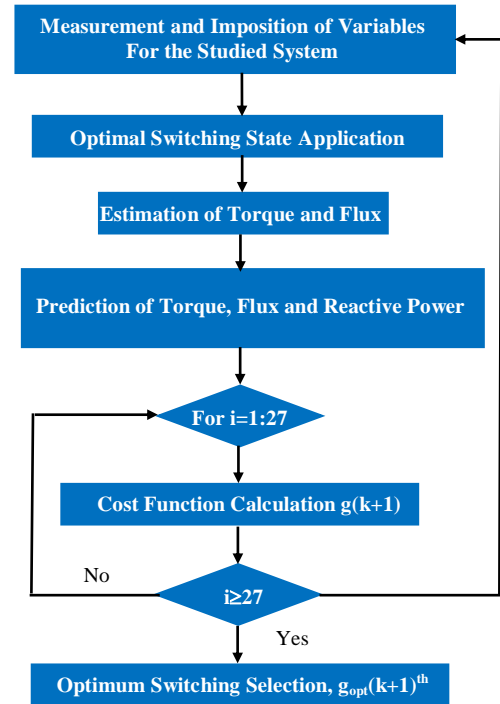


Fig. 3. Flowchart of the considered predictive control law.

VI. RESULTS AND DISCUSSION

For the evaluation of the effectiveness of the proposed models and PDTC algorithms of the power source connected WECS, extensive simulations are performed in MATLAB/Simulink[®] package program using SimPower Systems Library. The simulation processed and adopted a wind speed sequence as shown in Fig. 4. This variation of the wind is intended to give an evaluation of the response of the studied wind system in situations below and above the nominal wind speed.

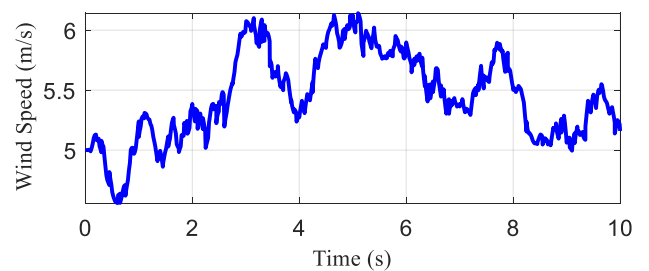


Fig. 4. Wind speed evolution.

According to the obtained results, the simulated control system successfully tracked the maximum available power of the wind turbine along the wind speed profile. Through Fig.5, it is noticed that the power coefficient is near to its appropriate value ($C_p^{max}=0.48$).

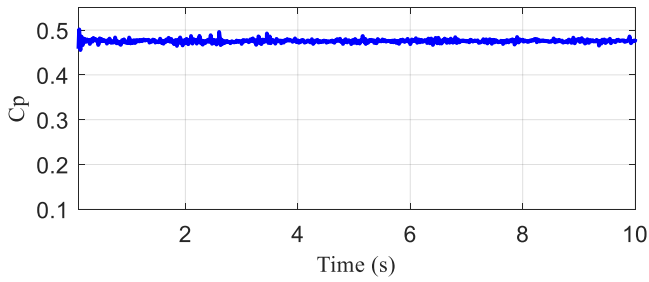


Fig. 5. Coefficient of the power.

The extracted mechanical power is also shown in Fig. 6. Notice that the mechanical power and the wind speed are correlated. Fig. 7 presents the stator flux ψ_s , it is obvious that the stator flux reaches its desired reference ψ_{ref} in good conditions, even when there are changes in the wind speed.

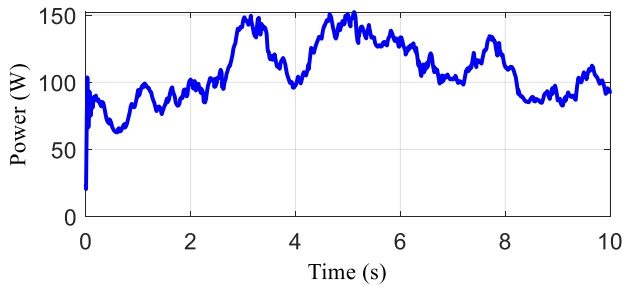


Fig. 6. Wind turbine power.

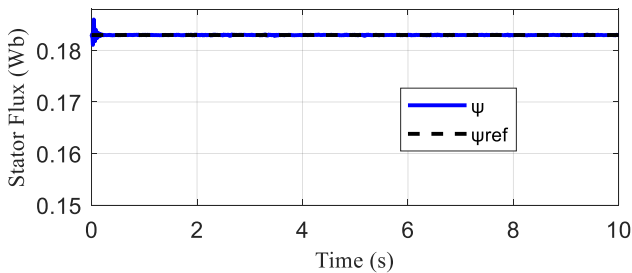


Fig. 7. Stator flux.

Fig. 8 depicts the simulation waveform of the $d-q$ axis stator currents of the PMSG. We observe through this figure that the stator current for the d axis is zero while it is proportional to the extracted mechanical power for the q axis. Fig. 9 shows the instantaneous three phase stator currents of the PMSG. As seen from the figure the three phase stator currents waveforms are nearly sinusoidal with a low total harmonic distortion (THD_i). A zoomed view of Fig. 9 is also given in Fig. 10.

Figs. 11 and 12 show the three-phase output voltage and current waveforms at the utility grid side respectively before filtering. As it's clearly shown, the output voltages and currents wave shapes is non-sinusoidal and it contains harmonics.

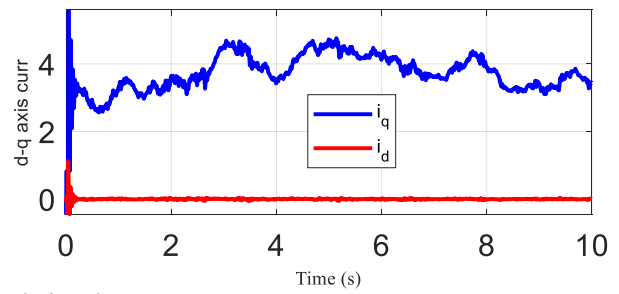


Fig. 8. $d-q$ axis currents.

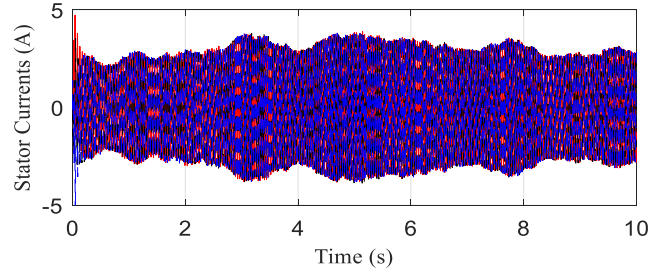


Fig. 9. Stator currents.

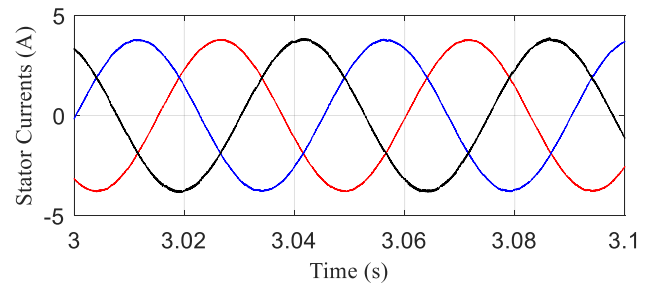


Fig. 10. Zoomed view of the stator currents.

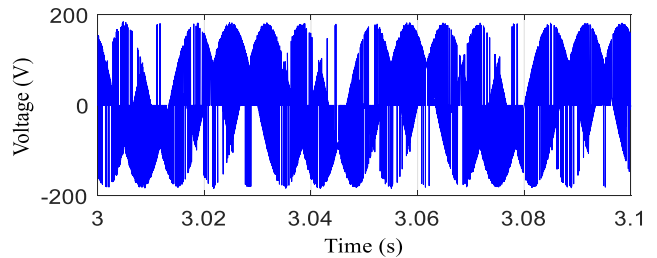


Fig. 11. Output phase voltage of the matrix converter.

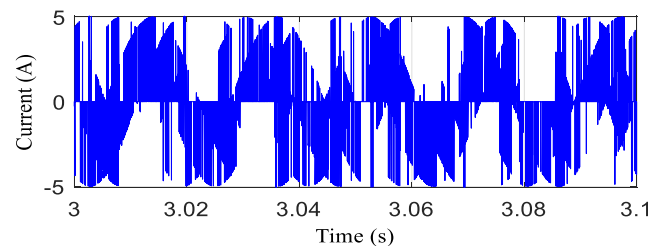
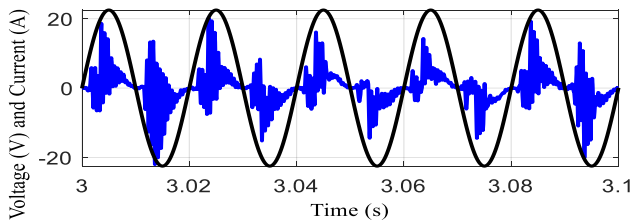
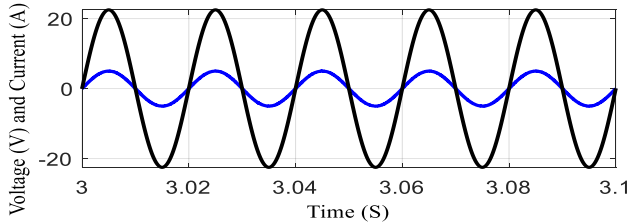


Fig. 12. Filter input currents.

Fig. 13 and Fig. 14 show the results without and with output factor correction respectively. Good grid-side behavior is recorded for these two cases but still show significant differences. With the implementation of the strategy with $\lambda_q=0$, the grid current is characterized by high distortion and phase shift with its phase voltage. Deploying the added term for output factor mastery while considering $\lambda_q>0$, we notice that the current is very near to the sinusoidal shape as shown in Fig. 14.

Fig. 13. Source voltage and current with $\lambda_q=0$.Fig. 14. Source voltage and current with $\lambda_q>0$.

The proposed study clearly shows that the intuitive approach for wind power generation systems has multiple advantages compared to the traditional wind system. The use of the DMC and PMSG allow to decrease the power stress and optimize the size of both the power converters and WECS.

VII. CONCLUSION

A wind energy conversion scheme containing a direct AC-AC matrix converter and model predictive control is presented in this paper. The torque and the flux of the PMSG is effectively controlled by the DMC to ensure a dual role of extracting the maximum power from the wind turbine under various wind speed situations as well as unity displacement power factor at the interface with the network. This task is important for a purely active power injection into the grid and an optimal utilization of the installed wind capacity. Due to the scheme of examination of the cost function by applying feasible switching state the proposed controller is superior to the commonly used PI regulator in that it does not require any supplementary modulation approaches or internal cascade control loops. Finally, the studied wind system with PMSG and matrix converter is successfully verified under MATLAB/Simulink environment. Via the obtained results, the suggested model and advanced control law can suitably follow the rotor speed reference to capture the maximum wind power whatever the wind speeds with minimization of the instantaneous reactive power at the interface with the power grid.

REFERENCES

- [1] M. Arifujjaman, "Reliability comparison of power electronic converters for grid-connected 1.5 kW wind energy conversion system," *Renewable Energy*, vol. 57, pp. 348–357, 2013.
- [2] A. Jahangiri and A. Radan, "Indirect matrix converter with unity voltage transfer ratio for AC to AC power conversion," *Electric Power Systems Research*, vol. 96, pp. 157–169, 2013.
- [3] S. Kahla, M. Bechouat, T. Amieur, M. Sedraoui, B. Babes and N. Hamouda, "Maximum power extraction framework using robust fractional-order feedback linearization control and GM-CPSO for PMSG-based WECS," *Wind Engineering*, vol. 45, no. 4, pp. 1040–1054, 2020.
- [4] H. Benbouhenni, N. Bizon, I. Colak, P. Thounthong and N. Takorabet, "application of fractional-order PI controllers and neuro-fuzzy pwm technique to multi-rotor wind turbine systems," *Electronics*, vol. 11, no. 9, pp. 1340–1366, 2022.
- [5] N. Hamouda, B. Babes, S. Kahla and Y. Soufi, "Real time implementation of grid connected wind energy systems: predictive current controller," *1st International Conference on Sustainable Renewable Energy Systems and Applications (ICSRESA)*, 2019.
- [6] M. Allouche, A. Sahbi, H. Ben Zina and M. Chaabane, "Novel fuzzy control strategy for maximum power point tracking of wind energy conversion system," *International Journal of Smart Grid*, vol. 3, no. 3, pp. 120–127, 2019.
- [7] R. Ika Putri, M. Rifa'i, S. Ika Noer and R. Ferdian, "Control of PMSG stand-alone wind turbine system based on multi-objectives PSO," *International Journal of Renewable Energy research*, vol. 10, no. 2, pp. 998–1004, 2020.
- [8] R. Melício, V.M.F. Mendes and J.P.S. Catalão, "Comparative study of power converter topologies and control strategies for the harmonic performance of variable-speed wind turbine generator systems," *Energy*, vol. 36, pp. 520–529, 2011.
- [9] O. Aissa, S. Moulahoum, I. Colak, B. Babes and N. Kabache, "Analysis, design and real-time implementation of shunt active power filter for power quality improvement based on predictive direct power control," *IEEE International Conference on Renewable Energy Research and Applications (ICRERA)*, pp. 79–84, 2016.
- [10] O. Aissa, S. Moulahoum, I. Colak, B. Babes and N. Kabache, "Analysis and experimental evaluation of shunt active power filter for power quality improvement based on predictive direct power control," *Environmental Science and Pollution Research*, vol. 25, no. 25, pp. 24548–24560, 2018.
- [11] N. Hamouda, H. Benalla, K. Hemsas, B. Babes and T. Ellinger, "Type-2 fuzzy logic predictive control of a grid connected wind power systems with integrated active power filter capabilities," *Journal of Power Electronics*, vol. 17, no. 6, pp. 1587–1599, 2017.
- [12] N. Hamouda, B. Babes, S. Kahla, Y. Soufi, J. Petzoldt and T. Ellinger, "Predictive control of a grid connected pv system incorporating active power filter functionalities," *1st International Conference on Sustainable Renewable Energy Systems and Applications*, 2019.
- [13] R. Bachar, A. Goléa and M.T. Benchouia, "The efficiency of current prediction controlled shunt active power filter based on three level inverter in balanced and unbalanced network cases," *International Journal of Engineering Science and Application*, vol. 1, no. 3, pp. 106–118, 2017.
- [14] V. Phuong, A.D. Tuan and N. Linh, "A novel multi-step model predictive control design for three-phase T-type inverter in grid-connected mode," *International Journal of Renewable Energy research*, vol. 11, no. 2, pp. 1968–1976, 2021.
- [15] M. Rivera, A. Wilson, A.C. Rojas, J. Rodriguez, R.J. Espinoza, W.P. Wheeler and L. Empringham, "A comparative assessment of model predictive current control and space vector modulation in a direct matrix converter," *IEEE Transactions on Industrial Electronics*, vol. 60, no. 2, pp. 578–588, 2013.
- [16] S. Vadi, F.B. Gürbüz, R. Bayindir and E. Hossain, "Design and simulation of a grid connected wind turbine with permanent magnet synchronous generator," *International Conference on Smart Grid (icSmartGrid)*, pp. 169–175, 2020.
- [17] Y.E. Abu Eldahab, N.H. Saad and A. Zekry, "Assessing wind energy conversion systems based on newly developed wind turbine emulator," *International Journal of Smart Grid*, vol. 4, no. 4, pp. 139–148, 2020.
- [18] A. Harrouz, I. Colak and K. Kayisli, "Energy modeling output of wind system based on wind speed," *IEEE International Conference on Renewable Energy Research and Applications (ICRERA)*, pp. 63–68, 2019.
- [19] S.H. Yusoff, N.S. Midi, S. Khan and M. Tohtayong, "Predictive control of AC/AC matrix converter," *International Journal of Power Electronics and Drive System*, vol. 8, no. 4, pp. 1932–1942, 2017.
- [20] M. Rivera, J. Rodriguez, J.R. Espinoza and H. Abu-Rub, "Instantaneous reactive power minimization and current control for an indirect matrix converter under a distorted AC supply," *IEEE Transactions on Industrial Informatics*, vol. 8, no. 3, pp. 482–490, 2012.
- [21] B. Babes, N. Hamouda, S. Kahla, H. Amar and S.S.M. Ghoneim, "Fuzzy model based multivariable predictive control design for rapid and efficient speed-sensorless maximum power extraction of renewable wind generators," *Electrical Engineering & Electromechanics*, no. 3, pp. 51–62, 2022.

